

Article

A Multicriteria Geographic Information System Analysis of Wildfire Susceptibility in the Andean Region: A Case Study in Ibarra, Ecuador

Paúl Arias-Muñoz , Santiago Cabrera-García  and Gabriel Jácome-Aguirre 

Laboratorio de Geociencias y Medio Ambiente (GEOMA), Carrera de Recursos Naturales Renovables, Facultad de Ingeniería en Ciencias Agropecuarias y Ambientales, Universidad Técnica del Norte (UTN), Avenida 17 de Julio 5-21 y Gral. José María Córdova, Ibarra EC100150, Ecuador; jscabrera@utn.edu.ec (S.C.-G.); gajacomea@utn.edu.ec (G.J.-A.)

* Correspondence: dparias@utn.edu.ec

Abstract: The uncontrolled spread of fire can have huge effects on ecosystems. In Ecuador, in 2022, wildfires caused a loss of 6566.66 hectares of vegetation cover. Ibarra is an Andean canton that has also been exposed to wildfires and their effects. The aim of this study was to map wildfire susceptibility in the Ibarra canton. Seven factors that directly affect these fires were examined: precipitation, temperature, water deficit, potential evapotranspiration, slope, proximity to roads, and land cover and land use. The variables were reclassified using Geographic Information Systems and a multicriteria analysis. The results showed that Ibarra has four susceptibility categories: very low, moderate, high, and very high. The more susceptible areas are those considered to have high and very high exposure, occupying 82% of the surface. Consequently, the most susceptible land covers are crops, pastures, shrub vegetation, and forests.

Keywords: multicriteria analysis; GIS; fire risk assessment; natural disasters; hazard mapping; Ibarra



Citation: Arias-Muñoz, P.; Cabrera-García, S.; Jácome-Aguirre, G. A Multicriteria Geographic Information System Analysis of Wildfire Susceptibility in the Andean Region: A Case Study in Ibarra, Ecuador. *Fire* **2024**, *7*, 81. <https://doi.org/10.3390/fire7030081>

Academic Editors: Kunpeng Yi and Shuai Yin

Received: 1 December 2023

Revised: 28 December 2023

Accepted: 4 January 2024

Published: 6 March 2024



Copyright: © 2024 by the authors. Licensee MDPI, Basel, Switzerland. This article is an open access article distributed under the terms and conditions of the Creative Commons Attribution (CC BY) license (<https://creativecommons.org/licenses/by/4.0/>).

1. Introduction

Different disturbances, including fires, can significantly impact the dynamics of ecosystems [1]. These fires cause the loss of individuals and biomass, which can occur suddenly or episodically, leading to alterations in the ecosystem's interrelationships [2]. Wildfires can spread across various ecosystems in rural areas and are not limited to a single land cover [3]. These fires are primarily categorized into human-ignited, anthropogenic, and naturally induced fires [4]. Human activities predominantly contribute to most wildfires on a global scale. For instance, in Europe, humans are responsible for an astounding 95% of all wildfires [5]. One direct consequence is the loss of natural vegetation cover. Fires are estimated to consume between 300 and 400 Mha (million hectares) of vegetation cover annually [6]. Wildfires pose a recurring problem in several regions worldwide, such as the Mediterranean region [7,8], Oceania [9], and North America [10]. The Andean region also faces this recurring issue, with wildfires becoming increasingly frequent during drought periods, affecting forest and vulnerable ecosystems such as paramos [11–15].

Wildfires have shifted from natural to anthropogenic origins exponentially, leading to increased fire events [16]. The anthropogenic origin can be attributed to various factors, such as land use changes [17], the characteristics of farming systems [18–20], population density and distribution [16,21], and accessibility [22]. Other factors that influence wildfire occurrence are associated with climate factors such as temperature, wind, or humidity [23,24]. In recent decades, climatic variables have become one of the most critical environmental problems, partly due to the impacts of climate variability and change [1,25]. Due to rising temperatures, the probability of vegetation cover suffering from ignition increases [24,26,27]. Topography and wind are also significant factors that influence fires, with fires spreading

faster on slopes [24,28,29]. However, the main cause that increases the likelihood of ignition is biomass burning by pasture, forest, and residue fires, which are carried out to convert new land for agricultural and livestock use [30,31].

Consequently, it is necessary to achieve efficient wildfire risk management to prevent their occurrence and recurrence [32]. One of the methods to efficiently manage this type of fire is the development of wildfire risk mapping [33,34]. Wildfire susceptibility maps can evaluate the favorable or unfavorable conditions a place presents for developing and spreading fires. For this reason, susceptibility mapping is used as a management tool in many countries worldwide, as it provides helpful information for prevention, not only to decision makers but also to the entire community in general [35].

Traditional in situ measurements are useful for assessing forest fire risk. However, they are costly and often inaccurate due to the human and economic resources required for their development [36]. The use of Geographic Information Systems (GISs) and remote sensing for the development of susceptibility mapping offers a more cost-effective solution than in situ methodologies and provides decision makers with precise information [11,28,37,38]. Consequently, this type of risk can be analyzed across large land areas using georeferenced information on the climatic, topographic, and biophysical variables involved in risk construction.

Several techniques and approaches have been developed in wildfire risk mapping [28, 37,39–41]. In recent years, fire risk has been modeled using GIS-based multicriteria decision analysis techniques [7,35,42]. Given the vulnerability of forest ecosystems to fire, GIS-MCDA methods not only generate information adapted to user-specific needs but also produce data that decision makers can easily comprehend. Various examples of MCDA methods can be found in the literature, such as the analytic hierarchy process (AHP) [35,40,42–44], the fuzzy AHP [45–47], the analytic network process [37,48], fuzzy logic [38], and artificial neural networks [39,49]. This study aims to address the existing knowledge gap concerning the threat that wildfires pose to Andean ecosystems. While several studies have been conducted on wildfire risk mapping, few have applied the AHP to the Andean region.

Some studies in Ecuador have mapped wildfire risk [50–54]. Ref. [53] used GIS data to identify the factors influencing the probability of forest fires in the country. The authors of [50], focusing on the Metropolitan District of Quito, not only determined the susceptible areas in the DMQ but also identified optimal management measures to reduce the danger, such as the location of the optimal routes for reaching the most dangerous areas. On the other hand, in the context of the Loja canton, located south of Ecuador, the authors of [54] determined that three machine learning techniques—logistic regression, logistic decision tree, and multivariate adaptive regression spline—could suitably identify areas susceptible to forest fires. These two studies are among the few developed in Ecuador to assess wildfire risk in Andean localities.

Considering that wildfires led to the loss of 6566.66 hectares of vegetation cover in Ecuador due to 1249 recorded incidents in 2022, the current investigations are indeed insufficient [55]. The Ibarra canton, the capital of the Imbabura Province, has experienced significant exposure to wildfires. Imbabura ranks among the top five provinces in Ecuador with the highest number of fires in 2022 [55]. Consequently, several hectares of natural vegetation in this territory have been lost. However, there are no studies on the area's susceptibility to this type of fire. Therefore, the main objective of this study was to develop a statistical model to map susceptibility to wildfires by using GIS data and conducting a multicriteria analysis in Ibarra, Ecuador. The model used in this study assigns weights to climatic and physical variables chosen for their practicality of application and their direct relationship with the occurrence of wildfires. Our central hypothesis is that this study's statistical susceptibility model behaves similarly to a map of the recorded hot spots and historic wildfires in the study area.

2. Materials and Methods

2.1. Study Area

Ibarra is an Andean canton located 115 km north of Quito with an area of 1105.56 km² (Figure 1). The canton is the capital of the Imbabura province, and it has five urban parishes (San Francisco, El Sagrario, Caranqui, Alpachaca, and Priorato) and seven rural parishes (San Antonio, La Esperanza, Angochagua, Ambuquí, Salinas, La Carolina, and Lita). San Antonio, La Esperanza, and Angochagua are rural parishes in the Andean zone. In contrast, the rural parishes of Lita and La Carolina are located in tropical areas.

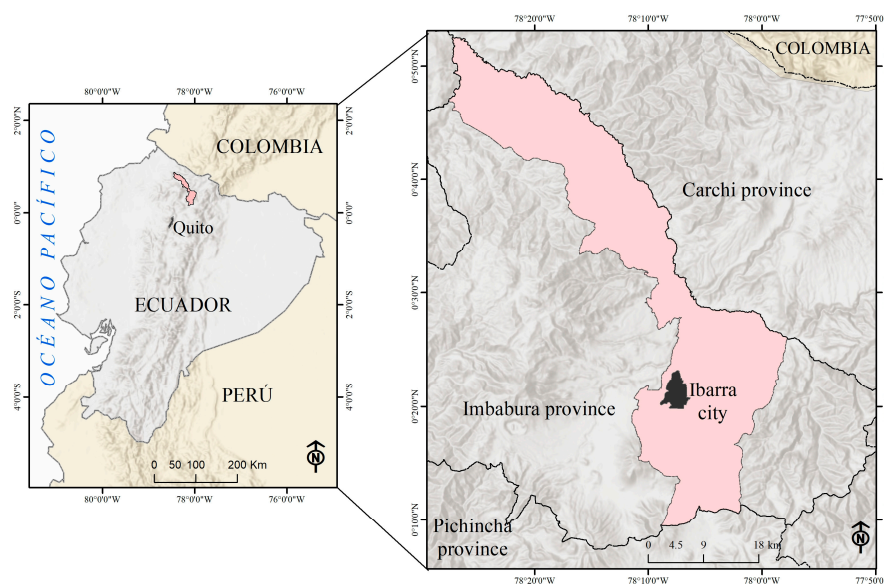


Figure 1. Location of the study area.

According to the authors of [56], this canton houses 217,469 inhabitants. The main productive activities are agricultural, industrial, and services, of which the most representative is the service sector, comprising 58% of the area's wholesale and retail trade activities. The industrial sector, centered around the manufacturing industry, represents 19.38%. Finally, the agricultural sector, with 11.61%, mainly involves the rural parishes Lita, La Carolina, and Salinas, with the main activities being associated with livestock, agriculture, forestry, and fishing [57].

Ibarra has an altitudinal range of 480 to 4500 m.a.s.l. and has average temperatures ranging from 4° to 23 °C. The climate in the canton is divided into three periods: one dry and two rainy seasons. The dry season is distributed between July and August, with precipitation of no more than 34.69 mm and temperatures of no less than 15.90 °C. The two rainy seasons take place between January–June and September–December, with precipitation values of 123.2 to 143.3 mm and temperatures between 16 and 16.29 °C [58].

2.2. Methods

The design of this study was non-experimental and cross-sectional, and it involved using spatially explicit models. The methodological process was divided into two sections: (a) the generation of the wildfire susceptibility model and (b) the validation of the model.

2.2.1. The Generation of the Wildfire Susceptibility Model

Conducting a literature review on global [59], regional [28], and local [24,50] aspects allowed us to identify some factors that condition wildfires. The Andean region is characterized by a mountainous topography in which an environmental mosaic usually develops (conditioned by micro-interactions between temperature, precipitation, slope, and/or terrain orientation) [60,61]. These factors influence forest structure, humidity, and fuel accumulation [61]. Therefore, factors grouped into physical and climatic factors were selected.

The climatic factors considered were water deficit, temperature, potential evapotranspiration (PET), and wind speed (Figure 2). Water deficit may serve as a more accurate variable to reflect the impact of accumulated precipitation on vegetation's water content, which can turn into fuel in a wildfire scenario [28,61]. Therefore, precipitation was not included. An increase in temperature leads to higher evapotranspiration, resulting in lower soil moisture and the land cover having an increased vulnerability to ignition [41]. This condition increases fire susceptibility due to the propensity of dry vegetation to ignite [28]. Wind speed influences a wildfire's intensity by reducing the vegetation's moisture content and supplying oxygen for combustion [62]. Additionally, wind plays a crucial role in controlling the spread of fires, which is influenced by an area's aspect and slope [24].

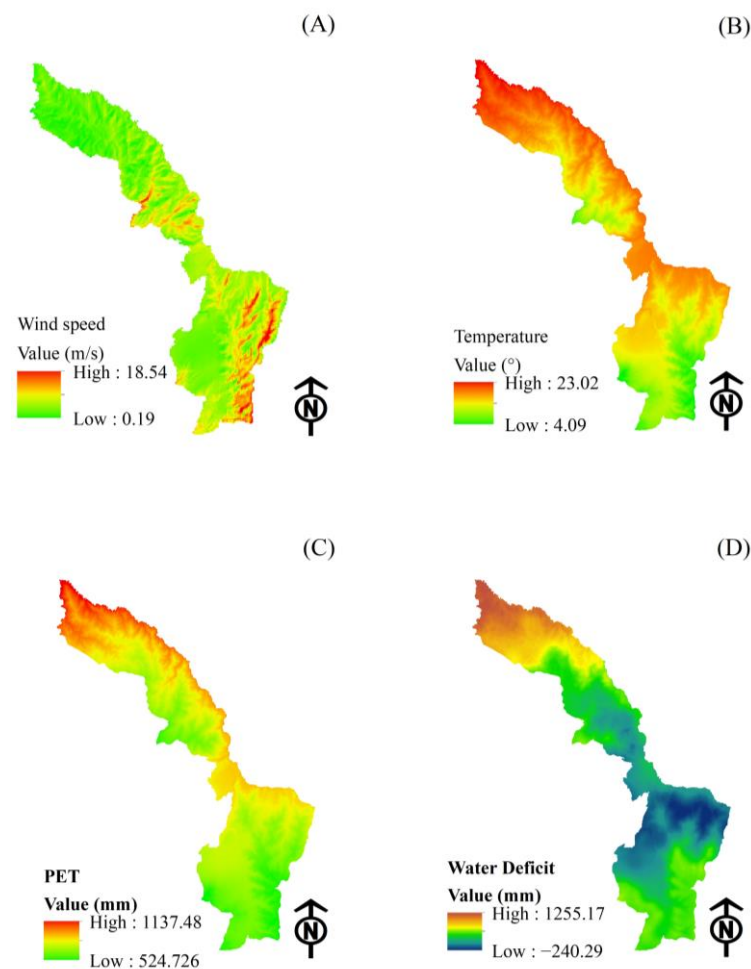


Figure 2. The climatic factors involved in wildfires; (A) is wind speed at a height of 50 m; (B) Mean temperature; (C) Potential evapotranspiration; (D) Water deficit.

On the other hand, the physical factors considered were slope, terrain orientation or aspect, land cover, road proximity, and the effect of burning efficiency (BE) (Figure 3). The last variable was expressed through the relative greenness index (RGI). BE is the percentage of total carbon released from the carbon pool contained in the aboveground biomass before combustion [63]. Some authors have shown that low air humidity and high temperatures can increase the burning efficiency because BE relates to land cover properties such as flammability, phenology and composition, vegetation structure, fine fuel moisture, or water content [64–66]. Topography influences the generation and dispersion of wildfires, so there is usually a link between fire, slope, and aspect [67]. The fire spread rate rises when the slope increases [68,69]. Aspect contributes to the susceptibility of a terrain to wildfire and its spread. For example, in contrast to west-facing slopes, east-facing slopes may receive

less rain during the rainy season in some equatorial areas due to wind and precipitation patterns. The result is that vegetation is more prone to wildfires than on eastern slopes with denser and wetter vegetation. In addition, in several regions of the world, it has been shown that there is a relationship between human activities and the occurrence of forest fires [67,70]. The shorter the distance to roads, the greater the probability of fire occurrence [61].

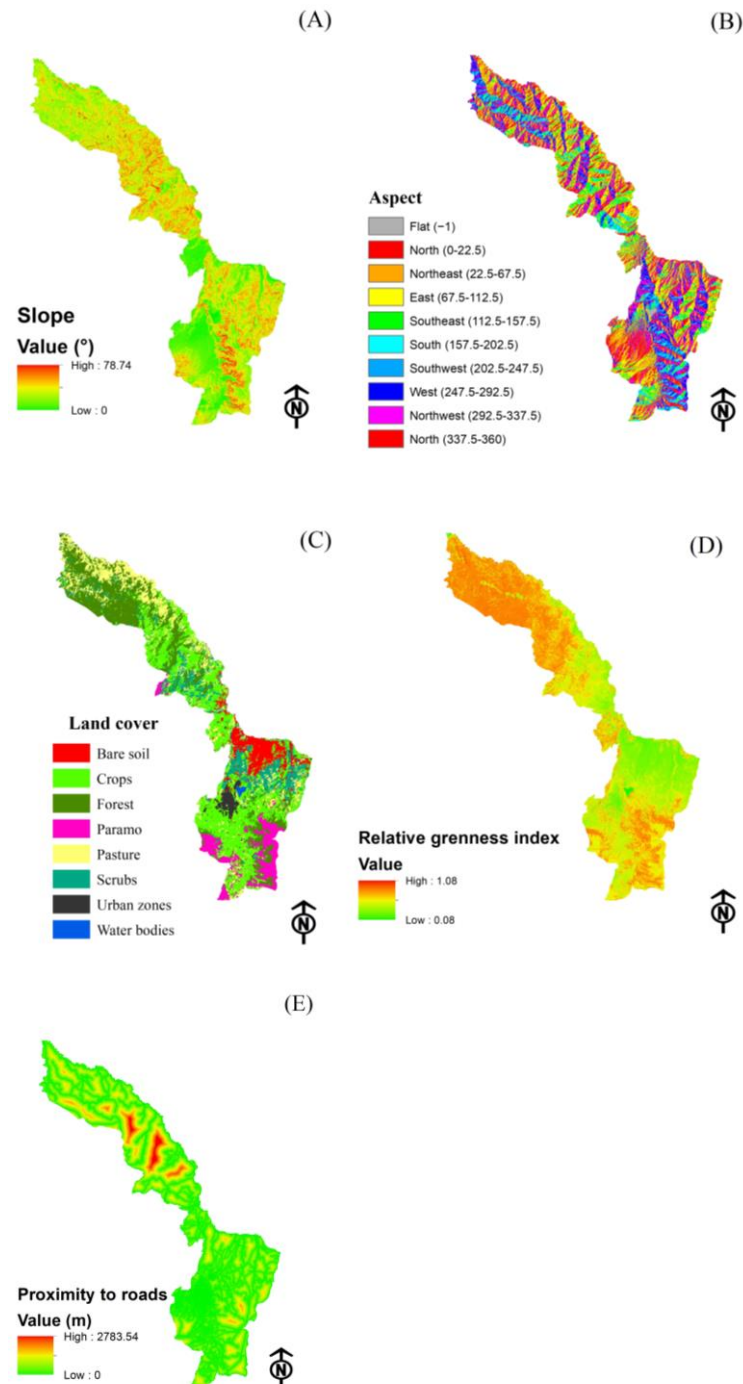


Figure 3. The physical factors involved in wildfires; (A) Slope of terrain; (B) Aspect; (C) Land cover; (D) Relative greenness index; (E) Proximity to roads.

Finally, each factor was reclassified according to the particular characteristics that contribute to the occurrence of fires. Therefore, five levels of susceptibility were established for each of them—very low, low, moderate, high, and very high—except for land cover,

for which a null category was also established. The susceptibility assignment process was carried out using the practical interval rule, where the mean would be plus one standard deviation or two standard deviations to determine the different susceptibility categories [71]. The values assigned to susceptibility were one for very low susceptibility, two for low susceptibility, three for moderate susceptibility, four for high susceptibility, and five for extreme susceptibility.

- Physical factors

Slope: The slope rating was obtained using the STRM-DEM in a Geographic Information System (GIS) with 30 m spatial resolution. The raster geodata were calculated in percentage units, and the reclassification of these data was performed by assigning ranges between 5% and 45% in five susceptibility levels [28] (Table 1).

Table 1. Slope classification for the city of Ibarra.

Value	Slope Ranges (%)	Susceptibility
1	<5	Very low
2	5–12	Low
3	12–25	Moderate
4	25–45	High
5	>45	Very high

Terrain orientation (Aspect): The terrain orientation was calculated using the DEM using a GIS. Aspect can influence wind behavior, water availability, and humidity. The susceptibility conditions based on the slope aspect for this equatorial zone were divided into the five classes presented in Table 2.

Table 2. Aspect classification.

Value	Aspect (°)	Susceptibility
1	Flat	Very low
2	West	Low
3	South, Southwest	Moderate
4	North, Northeast, Southeast, Northeast	High
5	East	Very high

Land cover: Sentinel 2B satellite images from 5 and 24 August 2018 were downloaded. These images were selected because they were the most recent images depicting the study area with no cloud cover. The imagery was calibrated and atmospherically corrected using QGIS software version 3.28.11. Then, relative topographic and geometric corrections were made to the images using the digital elevation model of the Radar Shuttle Topographic Mission (DEM-SRTM) with a final resolution of 30 m. These data were georeferenced to the study area using the WGS84 reference system, UTM projection, zone 17 South. Additionally, because Sentinel satellite images present a different spatial resolution to Landsat images, resampling was performed with the help of the neighbor-joining method, increasing the pixel size to 30 m [72].

To make the supervised classification, 160 real coordinates collected from Google Earth and validated in the field were used as reference data. Thus, 112 coordinates were used to generate the supervised LULC classification and 48 control points for validation (i.e., 70% of the reference data were used to create the cartographic model, and 30% of the reference data were used for validation). Thus, eight land covers were obtained: forest, paramos, scrubland, crops, pasture, urban areas, water bodies, and bare soil.

Validation was performed by applying the following statistical analyses: global classification precision (PG), user precision (PU), and producer precision (PP). The PG is the

percentage of correctly classified samples within a confusion matrix. It is calculated by dividing the total number of correctly classified pixels by the total number of reference pixels [73]. PU expresses the commission accuracy of the classification; in other words, it delivers information on how often the classified observations belong to that class or category. The PP or omission accuracy determines the percentage of actual observations of a particular category correctly classified on the map [74]. For each land cover and land use, classification accuracy was determined using the producer accuracy and user accuracy methods [73,75] (Table 3). Finally, fire susceptibility categories were assigned based on the information compiled after consultation with the eleven experts mentioned above (Table 4).

Table 3. Land cover validation.

Year	2018	
Cover	PP (%)	PU (%)
1	85.71	100
2	100	100
3	100	100
4	45.45	100
5	100	100
6	100	33.33
7	100	62.50
8	100	100

Abbreviations: 1 represents bare soil; 2 represents forest; 3 represents water bodies; 4 represents crops; 5 represents paramos; 6 represents pastures; 7 represents scrubs; 8 represents urban zones.

Table 4. Land cover classification.

Value	Land Cover	Susceptibility
0	Waterbodies and Urban zones	Null
3	Forest	Moderate
4	Pastures and Scrubs	High
4	Crops and Paramos	Very high

Relative greenness index (RGI): RGI was calculated as a function of the Normalized Difference Vegetation Index (NDVI) and expressed the burning efficiency (BE) [66]. NDVI measures the indirect effect of water loss, mainly changes in leaf area and plant chlorophyll content, so it is also considered sensitive to variations in plant water content [76]. NDVI is commonly employed as a proxy of fuel for analyses of fire occurrence [41]. This premise is the basis for considering that relative variations in NDVI can estimate BE, as presented in Equation (1). BE is presented as an inverse function of the relative variation in NDVI, which finally derives the relative greenness index (RGI) [77,78]. NDVI was calculated with Equation (2). Finally, susceptibility was assigned through the practical rule of the interval in the five susceptibility levels because zones with higher RGI are more likely to have wildfires (Table 5).

$$RGI_i = \frac{NDVI_i - NDVI_{min}}{NDVI_{max} - NDVI_{min}} \tag{1}$$

$$NDVI = \frac{NIR - Red}{NIR + Red} \tag{2}$$

where $NDVI_i$ corresponds to the NDVI value of a single period i . $NDVI_{min}$ and $NDVI_{max}$ are the minimum and maximum values NDVI, respectively. RGI is the relative greenness index (shown in percentage). NIR (or near-infrared) is the reflectance value in the near-infrared channel of the image, and Red is the reflectance value in the red channel of the image.

Table 5. Relative greenness index classification.

Value	RGI Ranges	Susceptibility
1	<0.55	Very low
2	0.55–0.67	Low
3	0.67–0.79	Moderate
4	0.79–0.91	High
5	0.91–1.08	Very high

Proximity to roads: Data from the road network were obtained from Open Street Map. The proximity to roads was calculated using the Euclidean distance tool in the ArcGIS software version 10.8.2. The distance from each pixel of the road network to the nearest source of a recorded fire outbreak was determined. Finally, five levels of susceptibility were determined through the practical rule of the interval, where the shortest distances have extreme susceptibility and the farthest distances have very low susceptibility (Table 6).

Table 6. Classification of proximity to roads.

Value	Ranges of Proximity to the Tracks (Meters)	Susceptibility
1	>200	Very low
2	150–200	Low
3	100–150	Moderate
4	50–100	High
5	<50	Very high

- Climatic factors

Mean temperature: A raster geodata of monthly mean data from 1970 to 2000 was also obtained from the WorldClim database [79] to keep the same period as precipitation. The data were projected to zone 17 South and delimited to the study area. We generated a temperature raster geodatabase with 30 m of spatial resolution, which performed a statistical downscaling process using SAGA GIS software, using altitude as a predictor variable. Finally, susceptibility was assigned through the practical rule of the interval in the five susceptibility levels because places with higher temperatures are more likely to have fires [24,51,80] (Table 7).

Table 7. Temperature classification.

Value	Temperature Ranges	Susceptibility
1	<8.5	Very low
2	8.5–12.5	Low
3	12.5–16	Moderate
4	16–20	High
5	>20	Very high

Wind speed: Strong winds can spread fire rapidly through dry vegetation, even changing the direction that a fire spreads in, according to aspect [41]. Wind speed information was downloaded from the World Wind Atlas at a height of 50 m and a spatial resolution of 282 m [81]. The wind speed was selected at a height of 50 m because the vegetation in this Andean zone typically fluctuates between 0.2 m and 30 m. There are *carex sp* species (0.2 m) in the paramos and *cedrela sp* species (30 m) in the humid tropical forests in the lower part of the north of the canton.

The downloaded data were projected to WGS84 17S and resampled to a 30 m resolution, corresponding to the SRTM resolution. This conversion involved using the nearest neighbor resampling algorithm with a resample tool in ArcGis software version 10.8.2. Finally, the susceptibility was assigned using the practical rule of the interval in the five

levels of susceptibility based on the fact that there is a greater probability of fire occurrence where there is higher wind speed (Table 8).

Table 8. Wind speed.

Value	Wind Speed Ranges	Susceptibility
1	0.18–2	Very low
2	2–4	Low
3	4–6.5	Moderate
4	6.5–9	High
5	>9	Very high

Potential evapotranspiration (PET): The method outlined in [82] was used to calculate PET by applying Equations (3)–(7), and Table 9. The susceptibility categories were established using the practical interval rule (Table 10).

$$ETP_{Tho} = e * L \tag{3}$$

where:

e = unadjusted monthly evapotranspiration (mm/month).

L = correction factor, established for latitude 0°, according Table 7.

Table 9. Correction factor.

Month	1	2	3	4	5	6	7	8	9	10	11	12
Latitude	1.04	0.94	1.04	1.01	1.04	1.01	1.04	1.04	1.01	1.04	1.01	1.04

Table 10. Classification of PET.

Value	Ranges PET	Susceptibility
1	<639	Very low
2	639–759	Low
3	760–881	Moderate
4	882–1003	High
5	>1003	Very high

$$e = 16 * \left(10 * \frac{tm}{I} \right)^a \tag{4}$$

where:

e = unadjusted monthly evapotranspiration (mm/month).

tm = monthly average temperature (°C).

I = annual heat index.

a = variable set.

$$ij = \left(\frac{tm}{5} \right)^{1.514} \tag{5}$$

where:

ij = Monthly heat index.

tm = Monthly temperature in °C.

$$I = \sum_{i=0}^n ij \tag{6}$$

$$a = 0.000000675 * I^3 - 0.0000771 * I^2 + 0.01792 * I + 0.49239 \tag{7}$$

Water deficit: This factor was determined based on the water balance calculation using the method outlined in [83]. Negative values are considered deficits, and positive values

are considered surpluses (Equation (8)). Therefore, where there is a water deficit, there is a greater probability of fire occurrence [61].

$$DH = P - PET \tag{8}$$

where:

DH = water deficit.

P = average precipitation.

PET = potential evapotranspiration.

Susceptibility was established through the use of the interval rule of thumb, and five categories were determined (Table 11).

Table 11. Classification of water deficit.

Value	Ranges PET	Susceptibility
1	>969	Very low
2	643–969	Low
3	317–643	Moderate
4	317–0	High
5	<0	Very high

- Wildfire susceptibility equation

To generate the susceptibility equation, we used the hierarchical multicriteria analysis (AHP), a technique developed by the authors of [84] based on the multicriteria technique to classify the different categories. The importance levels of the criteria were estimated using paired comparisons and a scale outlined by the authors of [84], which is shown in Table 12. The AHP was applied for the comparison of the eight selected variables. The relative importance of the susceptibility variables was analyzed by comparing two factors simultaneously. Those representing susceptibility situations were considered more relevant to measure the hierarchy among the factors/indicators. For this purpose, a double-entry matrix was constructed, with the factors in rows and columns, a main diagonal with a value equal to 1, and the relative weight of the comparison in each cell (Table 13). For example, temperature is considered to be a more critical factor than slope in defining susceptibility; therefore, the factor “temperature” was assigned the value “7”, and slope the inverse value was assigned a value of “1/7”. The vertical and horizontal averages of the paired comparison were calculated, and finally, the multicriteria weighting by factor was obtained.

Equations (9) and (10) were used to determine V_p and C_i [85]:

$$V_p = \sqrt[k]{W_1 * W_2 * W_3 * \dots * W_k} \tag{9}$$

$$C_i = \frac{V_{p_i}}{V_{p_i} + \dots + V_{p_k}} \tag{10}$$

where k = number of variables, and W = ratings.

The coherence coefficient (CR) was calculated according to Equations (11)–(13) in order to validate the calculated weighted weights. Thus, for the equation to be considered validated, the value of CR must be less than 0.10.

$$CR = \frac{CI}{R_{ci}} \tag{11}$$

$$CI = \frac{\lambda_{max} - n}{(n - 1)} \tag{12}$$

$$R_{ci} = \frac{1.98 * (n - 2)}{n} \tag{13}$$

where λ_{\max} is the maximum Eigenvalue of the matrix, n is the number of variables used, and Rci is the so-called random consistency index. This value depends on the number of elements being compared.

Table 12. Scale used for pairwise comparisons.

Score	Definition
1	Equal importance of one over the other
3	Moderate importance
5	Essential or strong importance
7	Very strong importance
9	Extreme importance
2, 4, 6, 8	Intermediate values among two judgements

Table 13. Pairwise comparison matrix.

	C1	C2	C3	C4	C5	C6	C7	C8	C9	Vp	Ci	λ_i
C1	1	1/7	5	3	3	1/4	5	1/5	1/4	0.90	0.08	1.69
C2	7	1	7	5	3	1/2	5	2	1/2	2.31	0.20	0.79
C3	1/5	1/7	1	2	1/5	1/3	2	1/7	1/5	0.39	0.03	0.97
C4	1/3	1/5	1/2	1	3	1/2	4	1/5	1/2	0.65	0.05	1.13
C5	1/3	1/3	5	1/3	1	1/2	5	1/3	1/2	0.75	0.06	0.98
C6	4	2	3	2	2	1	5	3	2	2.42	0.21	0.68
C7	1/5	1/5	1/2	1/4	1/5	1/5	1	1/7	1/7	0.25	0.02	0.73
C8	5	1/2	7	5	3	1/3	7	1	3	2.31	0.20	1.18
C9	4	2	5	2	2	1/2	7	1/3	1	1.79	0.15	0.62
Σ	22.06	4.02	29.00	20.58	15.40	3.28	34.00	6.02	4.09	11.77	1.00	8.77

Abbreviations: C1 represents slope, C2 represents temperature, C3 represents potential evapotranspiration, C4 represents the relative greenness index, C5 represents the wind speed, C6 represents land cover, C7 represents proximity to roads, C8 represents orientation terrain, C9 represents water deficit, Vp is the Eigenvector, Ci is the weighting coefficient for each variable, and λ_i is the Eigenvalue.

The wildfire susceptibility equation (Equation (14)) was the product of the weighted sum of the nine predictors.

$$\begin{aligned}
 WF = & (0.08 \times \text{Slope}) + (0.18 \times \text{Temp}) + (0.06 \times \text{PET}) + (0.07 \times \text{RGI}) \\
 & + (0.06 \times \text{Wspeed}) + (0.20 \times \text{Cov}) + (0.03 \times \text{Roads}) \\
 & + (0.17 \times \text{Aspect}) + (0.14 \times \text{Def})
 \end{aligned}
 \tag{14}$$

where WF = Wildfire Model Susceptibility; Slope = reclassified slope; Temp = reclassified temperature; PET = reclassified potential evapotranspiration; RGI = the relative greenness index; Wspeed = wind speed; Cov = reclassified land cover; Roads = the reclassified Euclidean distance of the roads; Aspect = reclassified aspect; Def = reclassified water deficit.

The calculated CI was 0.13, which was then divided by the Rci (1.54) to obtain a value of CR = 0.088. Thus, the consistency ratio is lower than 0.10. Thus, the model is suitable. Based on Equation (14), the map algebra technique was applied based on the developed matrix process, and the preliminary wildfire model was generated in a GIS environment. The geospatial information was used with a uniform spatial resolution of 30 m because this is a suitable pixel size for geospatial analysis [86]. Therefore, the selected variables had spatial information available at 30 m resolution, and their resampling could be carried out without causing territorial distortion. Once the preliminary wildfire susceptibility mapping was completed, the map was filtered by eliminating isolated pixels that did not represent anything relevant to our study. The wildfire susceptibility map was generated, validated with heat spots, and divided into susceptibility categories. The maximum and minimum values obtained after applying Equation (13) for wildfire susceptibility were considered to define the susceptibility categories. These values are 5 and 0, respectively, considering

that water bodies and urban areas have a null susceptibility to this type of fire. Finally, the susceptibility was presented in five classes divided into equal intervals: very low, low, moderate, high, and very high [28,37].

2.2.2. Susceptibility Model Validation

The model was validated using heat spots from the Brazilian National Institute for Space Research (INPE) portal. The INPE has a database of heat spots for South America from 1998, and for Ecuador, data dating back to 2000 can be obtained. For the study area, information dating back to 1 January 2023 until 22 October 2023 was used, corresponding to the AQUA, GOES, NOAA, TERRA, ATSR, and TRMM satellites. The information on the heat spots was spatially crossed with the categories of high and extreme susceptibility, and the following hypothesis was tested: a) there are similarities or associations between the model obtained and the hot spots (they are associated). Verification was carried out by applying the ROC curve's low area. The latter analysis achieves the highest accuracy when the values are closer to one (1) [87]. A Receiver Operating Characteristic (ROC) curve was used to determine the accuracy of the wildfire susceptibility map [35,37,43,48,49]. This method allows one to analyze the true-positive and false-positive values at each curve point. The Area Under the Curve (AUC) can be classified into five categories: 1 to 0.9 = excellent, 0.9 to 0.8 = very good, 0.8 to 0.7 = good, 0.7 to 0.6 = medium, and >0.6 = poor [37,88]. A flowchart based on this methodological background was prepared to simplify the understanding of our methodological process (Figure 4).

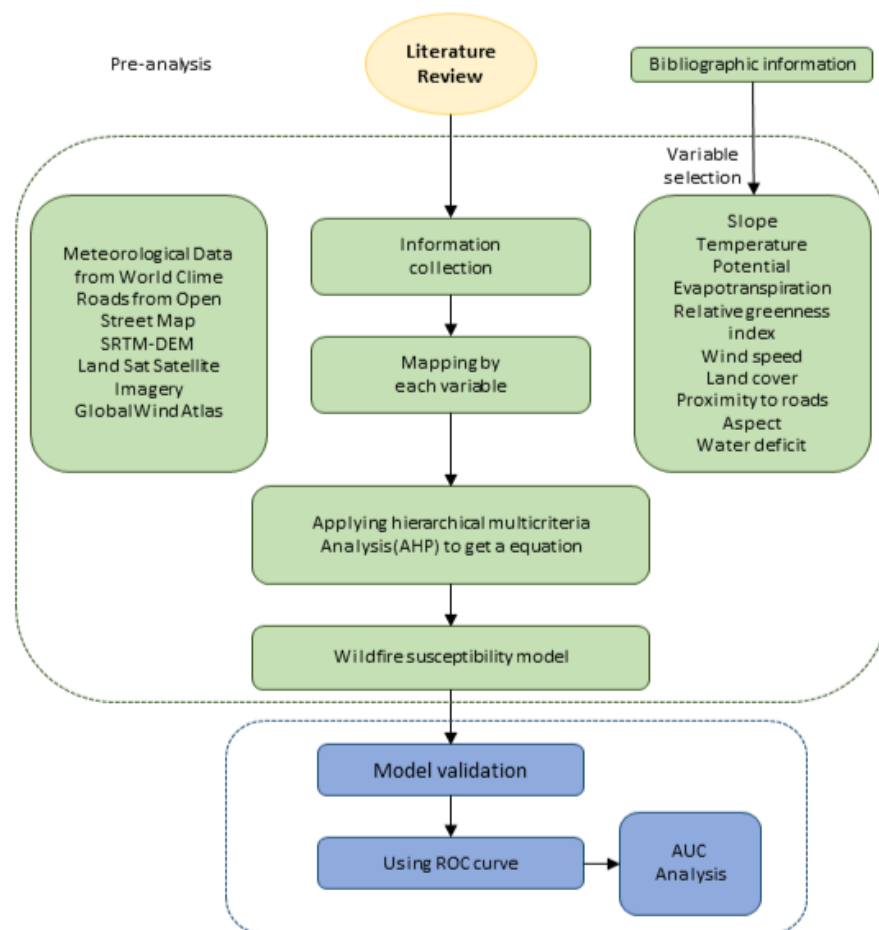


Figure 4. Methodology flowchart.

3. Results

The study area includes varying degrees of risk: approximately 104.54 km² (10%) is at very low risk, 83.13 km² (8%) at moderate risk, 886.90 km² (81%) at high risk, and 16.32 km² (1%) at very high risk, as shown in Figure 5. No low susceptibility areas were found in Ibarra. When the areas of high and very high risk are combined, 82% of Ibarra canton is considered susceptible to wildfires. This susceptibility can be attributed to the fact that around 96% of Ibarra is covered by vegetation including forests, shrubs, pastures, and crops, as depicted in Figure 3c.

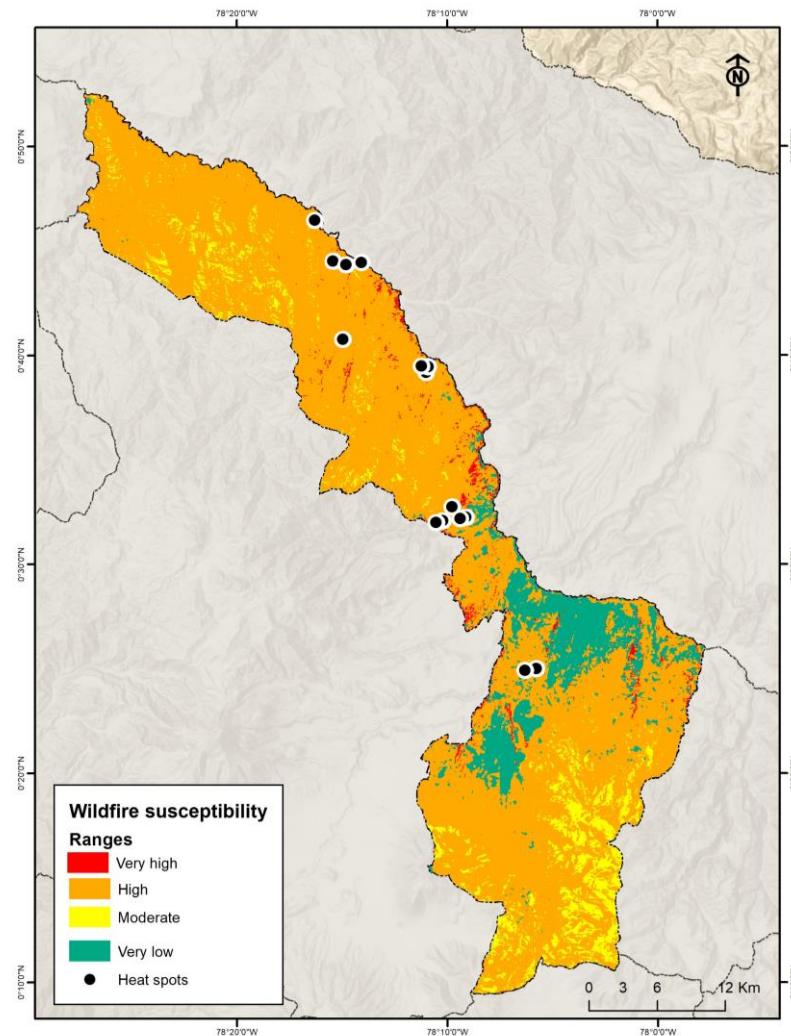


Figure 5. A map of wildfire susceptibility in the Ibarra canton.

Model Validation

In this study, a ROC curve was used to estimate the accuracy of the fire susceptibility map generated using the AHP (Figure 6). Our statistical validation (AUC = 0.96) shows that the model is acceptable and excellent, since there is an association between the location of hot spots and the areas with high and very high susceptibility to fires (as predicted by the model). Other wildfire susceptibility models show ROC curves with accuracy values of 77.5% [35], 82% [37], and 92.4% [48]. We recommend that this model be adapted to subtropical, tropical, and equatorial regions, considering that variables must be adapted to the local climate.

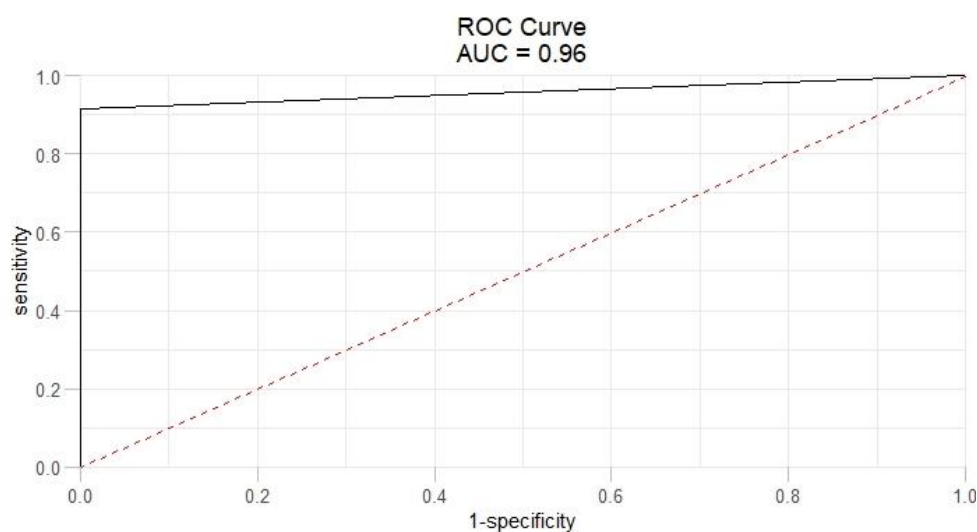


Figure 6. The ROC curve of the wildfire susceptibility model.

4. Discussion

Areas of high and very high susceptibility are widespread across the territory, except for urban areas, water bodies, eastern zones dominated by bare soils, and southeastern zones where paramos constitute the primary cover. The pattern of high and very high susceptibility aligns with regions characterized by high temperatures, natural cover, and steep slopes, all of which contribute to the propagation of fires. The average temperature in the Ibarra canton is 15° approximately; however, areas with high susceptibility exceed 16.30° . Consequently, areas susceptible to fire are those where the average temperature exceeds the canton's average temperature. There is a strong correlation between the rise in temperature and the incidence of forest fires, similar to the correlation with potential evapotranspiration [28,35,46].

At the same time, as the area's water deficit rises, so does its susceptibility to fires. When water availability drops below 394 mm within the vegetation cover, the fire risk escalates. This is due to the inverse correlation between the amount of precipitation and the risk of wildfires [51]. In Ibarra, susceptibility values decrease as precipitation increases. When precipitation is less than 810 mm, there is high fire susceptibility, while when it is higher than 891 mm, there is low fire vulnerability.

Regarding slope, it was concluded that the frequency of forest fires was higher on slopes greater than 35% [28]. Fire risk increases as the degree of the slope increases, because the inclination favors the ascent of hot air and fire propagation is affected by the accumulation of heat [46,68,69]. In addition, it was determined that the distance to roads is indeed a predictive factor that influences the occurrence of forest fires. This suggests that proximity to population centers or anthropic activities impacts fire susceptibility [35]. The presence of communication routes tends to encourage human activity, which is often considered a trigger for such fires [89–91].

In the study area, the climatic variables not only directly influence the origin of these events but also impact the development of human activities, particularly agriculture. Notably, during the dry season months of July and August, when land is prepared for agricultural planting, there is a surge in the frequency of forest fires. This is corroborated by data from the National Risk Secretariat, which indicates that 26% of the fires recorded in the city of Ibarra in 2020 occurred during these months.

On the other hand, there are few areas in the canton with very low susceptibility which are concentrated in urban areas. The absence of vegetation cover, except in parks or avenues, means susceptibility is almost null. There are also a few areas with moderate susceptibility which are concentrated in the southeast and southwest, where paramos are abundant. A paramo is defined as an ecosystem with a typical tropical high mountain climate and low

temperatures since their average temperature is around 7°, with moderate precipitation characterized by low rainfall intensities, which vary between 700 and 3000 mm [92–94]. However, the moderate fire susceptibility of the paramo in the canton under study can be attributed to the presence of wind. The wind, which can be quite strong and highly variable in direction, is influenced by the area's steep slopes and rugged topography [93].

Overall, natural land covers are susceptible to fire due to their lack of adaptive strategies to this phenomenon. However, certain land covers, such as the rainforest, are exceptions due to their unique climatic conditions [12]. Temperature, on the other hand, regulates the moisture content of the fuel in such a way that it decreases the humidity and increases the probability of ignition and propagation [95]. Another variable that directly influences the high susceptibility of the canton is the water deficit because, according to [61], when it rises, the fuel moisture reduces and ignition probability increases.

In sectors with high or very high susceptibility, numerous studies have indicated the possibility of implementing a series of actions and strategies to help reduce or mitigate fires [16,96–98]. According to the particular geographical and socioeconomic conditions of the human settlements and ecosystems of the Andean region, it is considered that the implementation of some strategies would be complex or unfeasible, especially in the Ibarra canton, where land use, temperature, and slope orientation are key factors in the spread of fires; the most viable strategies would be firebreaks, observation towers, and the implementation of measures based on technical scientific data [16]. In the fight against forest fires, firebreaks are essential to contain the spread of fires and protect communities and ecosystems [98]. However, in the Andean region, the feasibility of this strategy presents unique challenges due to the region's geographical and socioeconomic contexts. The mountainous topography of the Andean region can make it challenging to create effective firebreaks, as the construction of defense lines in steep terrain can be costly and logistically complicated [96]. In addition, climate variability in the region (enhanced by climate change), including heavy rainfall and prolonged droughts, complicates firebreak planning and maintenance. From a socioeconomic point of view, a lack of resources and pressure on land use can also limit the successful implementation of firebreaks. Local communities often rely on agriculture and livestock, making land allocation for firebreak creation a sensitive issue [16]. Overcoming these challenges may require a comprehensive strategy involving local communities, government agencies, and environmental organizations. Specifically, environmental (interdisciplinary and multicultural) education on fire management, the careful planning of firebreak locations, and adaptability to changing climatic conditions are essential to maximize the effectiveness of this strategy in the Andean region.

Installing observation towers for the early detection of forest fires in the Andean region is a viable and valuable proposal. The high altitudes of the Andean mountains can offer strategic locations for these towers, improving visibility. However, topographical challenges such as the difficulties regarding access to some remote areas and extreme weather conditions could affect their effectiveness. In addition, the need for investment in infrastructure, technology, and the training of local personnel and their salaries could condition their implementation and viability [99]. Despite these challenges, observation towers represent a crucial tool for ensuring rapid and efficient responses to forest fires and could be one of the first measures to be implemented [6]. Finally, implementing technical and scientific strategies to mitigate fires in the Andean region is essential and feasible [100]. They would allow decision makers to be continuously fed with accurate information on weather patterns, vegetation, and fire risks, helping them in implementing effective policies and preventive measures [97]. However, some geographical challenges, such as topographic diversity, require an adaptive approach to collect accurate data. Furthermore, in a socioeconomic context where resources may be limited, investment in monitoring technologies and scientific capacities could be a constraint [101]. Collaboration between governments, scientific institutions, and local communities could be key to overcoming these challenges and effectively implementing evidence-based measures that reduce fire risk and protect valuable Andean ecosystems [96].

5. Conclusions

Overall, 82% of the Ibarra canton is highly and very highly susceptible to fires. The behavior of these types of susceptibility mainly coincides with high temperatures, natural cover, and steep slopes that favor the spreading of fires. The most susceptible land covers are crops, pastures, scrubs, vegetation, and forestry. Although the paramo within the canton is considered a very susceptible cover, the presence of low temperatures, high rainfall, and surplus water, as well as its accessibility difficulties, make the susceptibility in this ecosystem moderate. However, this does not mean that fires will not occur here, but rather that they are areas with a low probability of ignition that can maintain their combustion capacity in case of spread. This study confirms that fire susceptibility and spreading depends on different types of cover and that the appropriate term for these types of fire events is “wildfires”, not the commonly used term “forest fires”.

In sectors with high and very high susceptibility, we recommend the implementation of firebreaks and the installation of watch towers at an altitude of 15 to 20 m to cover as much of the visual field as possible. The use of our data could be helpful for decision makers, and the application of these recommendations could prevent the annual recurrence of wildfires in the Ibarra canton. Finally, the wildfire susceptibility model used in this study, obtained through the GIS-assisted application of the aforementioned multicriteria methodology, is reliable because the susceptibility information provided coincides with the hot spots presented in this paper.

Author Contributions: Conceptualization, P.A.-M.; methodology, P.A.-M.; software, P.A.-M.; validation, P.A.-M. and G.J.-A.; formal analysis, P.A.-M., G.J.-A. and S.C.-G.; investigation, P.A.-M., G.J.-A. and S.C.-G.; resources, P.A.-M., G.J.-A. and S.C.-G.; data curation, P.A.-M.; writing—original draft preparation, P.A.-M.; writing—review and editing, P.A.-M. and G.J.-A.; visualization, P.A.-M., G.J.-A. and S.C.-G.; supervision, resources, funding acquisition, P.A.-M., G.J.-A. and S.C.-G. All authors have read and agreed to the published version of the manuscript.

Funding: This research was funded by the Centre of Research (CUICYT) of Universidad Técnica del Norte, Grant.

Institutional Review Board Statement: Not applicable.

Informed Consent Statement: Not applicable.

Data Availability Statement: The climate data used in this study are available at <https://worldclim.org/data/worldclim21.html> (accessed on 17 November 2023).

Acknowledgments: Universidad Técnica del Norte was the institution that contributed to funding this study by providing all the technological tools and grants to achieve the research objectives.

Conflicts of Interest: The authors declare no conflict of interest.

References

1. Flannigan, M.D.; Stocks, B.J.; Wotton, B.M. Climate Change and Forest Fires. *Sci. Total Environ.* **2000**, *262*, 221–229. [[CrossRef](#)] [[PubMed](#)]
2. Pereira, P.; Bogunovic, I.; Zhao, W.; Barcelo, D. Short-Term Effect of Wildfires and Prescribed Fires on Ecosystem Services. *Curr. Opin. Environ. Sci. Health* **2021**, *22*, 100266. [[CrossRef](#)]
3. Leuenberger, M.; Parente, J.; Tonini, M.; Pereira, M.G.; Kanevski, M. Wildfire Susceptibility Mapping: Deterministic vs. Stochastic Approaches. *Environ. Model. Softw.* **2018**, *101*, 194–203. [[CrossRef](#)]
4. Guo, F.; Su, Z.; Wang, G.; Sun, L.; Lin, F.; Liu, A. Wildfire Ignition in the Forests of Southeast China: Identifying Drivers and Spatial Distribution to Predict Wildfire Likelihood. *Appl. Geogr.* **2016**, *66*, 12–21. [[CrossRef](#)]
5. San-Miguel-Ayanz, J.; Schulte, E.; Schmuck, G.; Camia, A.; Strobl, P.; Liberta, G.; Giovando, C.; Boca, R.; Sedano, F.; Kempeneers, P.; et al. Comprehensive Monitoring of Wildfires in Europe: The European Forest Fire Information System (EFFIS). In *Approaches to Managing Disaster-Assessing Hazards, Emergencies and Disaster Impacts*; Tiefenbacher, J., Ed.; InTech: Ispra, Italy, 2012; ISBN 978-953-51-0294-6.
6. Robinne, F.-N.; Burns, J.; Kant, P.; Flannigan, M.; Kleine, M.; de Groot, B.; Wotton, D. *Global Fire Challenges in a Warming World*; IUFRO: Vienna, Austria, 2018.
7. Akbulak, C.; Tatlı, H.; Aygün, G.; Sağlam, B. Forest Fire Risk Analysis via Integration of GIS, RS and AHP: The Case of Çanakkale, Turkey. *J. Hum. Sci.* **2018**, *15*, 2127–2143. [[CrossRef](#)]

8. Pausas, J.G. Changes in Fire and Climate in the Eastern Iberian Peninsula (Mediterranean Basin). *Clim. Change* **2004**, *63*, 337–350. [[CrossRef](#)]
9. Harris, S.; Lucas, C. Understanding the Variability of Australian Fire Weather between 1973 and 2017. *PLoS ONE* **2019**, *14*, e0222328. [[CrossRef](#)]
10. Littell, J.S.; Peterson, D.L.; Riley, K.L.; Liu, Y.; Luce, C.H. A Review of the Relationships between Drought and Forest Fire in the United States. *Glob. Change Biol.* **2016**, *22*, 2353–2369. [[CrossRef](#)]
11. Avila Vélez, E.F. Propuesta Metodológica Para Cuantificar Áreas Afectadas Por Incendios Forestales Utilizando Imágenes Satelitales Sentinel-2. Caso de Estudio Páramo Del Almorzadero Colombia. *UD Y La Geomática* **2020**, *15*, 25–32. [[CrossRef](#)]
12. del Campo Parra-Lara, Á.; Bernal-Toro, F.H. Incendios de Cobertura Vegetal y Biodiversidad: Una Mirada a Los Impactos y Efectos Ecológicos Potenciales Sobre La Diversidad Vegetal. *El Hombre Y La Máquina* **2010**, *35*, 67–81. Available online: <https://www.redalyc.org/pdf/478/47817140008.pdf> (accessed on 3 January 2024).
13. Sarango-Cobos, J.; Muñoz, J.; Muñoz, L.; Aguirre, Z. Impacto Ecológico de Un Incendio Forestal En La Flora Del Páramo Antrópico Del Parque Universitario “Francisco Vivar Castro”, Loja, Ecuador. *Bosques Latid. Cero* **2019**, *9*, 101–114. Available online: <https://revistas.unl.edu.ec/index.php/bosques/article/view/687> (accessed on 3 January 2024).
14. Veblen, T.T.; Kitzberger, T.; Raffaele, E.; Mermoz, M.; González, M.E.; Sibold, J.S.; Holz, A. The Historical Range of Variability of Fires in the Andean-Patagonian Nothofagus Forest Region. *Int. J. Wildland Fire* **2008**, *17*, 724. [[CrossRef](#)]
15. Vergara, E.E.G.; Molina, M.A.C. Análisis Espacial de Incendios Forestales En La Provincia Del Azuay. *Polo Del Conoc. Rev. Científico-Prof.* **2020**, *5*, 337–361.
16. Úbeda, X.; Sarricolea, P. Wildfires in Chile: A Review. *Glob. Planet. Change* **2016**, *146*, 152–161. [[CrossRef](#)]
17. Butsic, V.; Kelly, M.; Moritz, M.A. Land Use and Wildfire: A Review of Local Interactions and Teleconnections. *Land* **2015**, *4*, 140–156. [[CrossRef](#)]
18. Amissah, L. Effects of Wildfire on Farming System Dynamics in the Fire-Prone Forest Belt of Ghana. Master’s Thesis, Kwame Nkrumah University of Science and Technology, Kumasi, Ghana, 2003.
19. Rodrigues Da Cunha, E.; Guimarães Santos, C.A.; Marques Da Silva, R.; Bacani, V.M.; Pott, A. Future Scenarios Based on a CA-Markov Land Use and Land Cover Simulation Model for a Tropical Humid Basin in the Cerrado/Atlantic Forest Ecotone of Brazil. *Land Use Policy* **2021**, *101*, 105141. [[CrossRef](#)]
20. Simmons, C.S.; Walker, R.T.; Wood, C.H.; Arima, E.; Cochrane, M. Wildfires in Amazonia: A Pilot Study Examining the Role of Farming Systems, Social Capital, and Fire Contagion. *J. Lat. Am. Geogr.* **2004**, *3*, 81–95. [[CrossRef](#)]
21. Sirca, C.; Casula, F.; Bouillon, C.; García, B.F.; Fernández Ramiro, M.M.; Molina, B.V.; Spano, D. A Wildfire Risk Oriented GIS Tool for Mapping Rural-Urban Interfaces. *Environ. Model. Softw.* **2017**, *94*, 36–47. [[CrossRef](#)]
22. Moreno, J.M.; Viedma, O.; Zavala, G.; Luna, B. Landscape Variables Influencing Forest Fires in Central Spain. *Int. J. Wildland Fire* **2011**, *20*, 678. [[CrossRef](#)]
23. Grillakis, M.; Voulgarakis, A.; Rovithakis, A.; Seiradakis, K.D.; Koutroulis, A.; Field, R.D.; Kasoar, M.; Papadopoulos, A.; Lazaridis, M. Climate Drivers of Global Wildfire Burned Area. *Environ. Res. Lett.* **2022**, *17*, 045021. [[CrossRef](#)]
24. Pazmiño, D. Peligro de Incendios Forestales Asociado a Factores Climáticos En Ecuador. *Fi* **2019**, *1*, 10–18. [[CrossRef](#)]
25. Abatzoglou, J.T.; Williams, A.P.; Boschetti, L.; Zubkova, M.; Kolden, C.A. Global Patterns of Interannual Climate–Fire Relationships. *Glob. Change Biol.* **2018**, *24*, 5164–5175. [[CrossRef](#)] [[PubMed](#)]
26. Schroeder, M.J. *Ignition Probability*; Rocky Mountain Research Station: Denver, CO, USA, 1969.
27. Vasilakos, C.; Kalabokidis, K.; Hatzopoulos, J.; Matsinos, I. Identifying Wildland Fire Ignition Factors through Sensitivity Analysis of a Neural Network. *Nat. Hazards* **2009**, *50*, 125–143. [[CrossRef](#)]
28. Eugenio, F.C.; Dos Santos, A.R.; Fiedler, N.C.; Ribeiro, G.A.; Da Silva, A.G.; Dos Santos, Á.B.; Paneto, G.G.; Schettino, V.R. Applying GIS to Develop a Model for Forest Fire Risk: A Case Study in Espírito Santo, Brazil. *J. Environ. Manag.* **2016**, *173*, 65–71. [[CrossRef](#)] [[PubMed](#)]
29. Macias Fauria, M.; Johnson, E.A. Climate and Wildfires in the North American Boreal Forest. *Phil. Trans. R. Soc. B* **2008**, *363*, 2315–2327. [[CrossRef](#)] [[PubMed](#)]
30. Crutzen, P.J.; Andreae, M.O. Biomass Burning in the Tropics: Impact on Atmospheric Chemistry and Biogeochemical Cycles. *Science* **1990**, *250*, 1669–1678. [[CrossRef](#)] [[PubMed](#)]
31. Mielnicki, D.M.; Canziani, P.O.; Drummond, J.; de los Procesos, P.D.E.; en el Cambio Global, A. Quema de Biomasa En El Centro-Sur de Sudamérica: Incendios Locales, Impactos Regionales. In *Anales IX Congreso Argentino de Meteorología*; Centro Argentino de Meteorólogos: Buenos Aires, Argentina, 2005.
32. Kc, U.; Hilton, J.; Garg, S.; Aryal, J. A Probability-Based Risk Metric for Operational Wildfire Risk Management. *Environ. Model. Softw.* **2022**, *148*, 105286. [[CrossRef](#)]
33. Gonzalez-Mathiesen, C.; Ruane, S.; March, A. Integrating Wildfire Risk Management and Spatial Planning—A Historical Review of Two Australian Planning Systems. *Int. J. Disaster Risk Reduct.* **2021**, *53*, 101984. [[CrossRef](#)]
34. Roberts, M.E.; Rawlinson, A.A.; Wang, Z. Ember Risk Modelling for Improved Wildfire Risk Management in the Peri-Urban Fringes. *Environ. Model. Softw.* **2021**, *138*, 104956. [[CrossRef](#)]
35. Sivrikaya, F.; Küçük, Ö. Modeling Forest Fire Risk Based on GIS-Based Analytical Hierarchy Process and Statistical Analysis in Mediterranean Region. *Ecol. Inform.* **2022**, *68*, 101537. [[CrossRef](#)]

36. Çolak, E.; Sunar, F. Evaluation of Forest Fire Risk in the Mediterranean Turkish Forests: A Case Study of Menderes Region, Izmir. *Int. J. Disaster Risk Reduct.* **2020**, *45*, 101479. [CrossRef]
37. Abedi Gheshlaghi, H.; Feizizadeh, B.; Blaschke, T. GIS-Based Forest Fire Risk Mapping Using the Analytical Network Process and Fuzzy Logic. *J. Environ. Plan. Manag.* **2020**, *63*, 481–499. [CrossRef]
38. Juvanhol, R.S.; Fiedler, N.C.; Santos, A.R.D.; Silva, G.F.D.; Omena, M.S.; Eugenio, F.C.; Pinheiro, C.J.G.; Ferraz Filho, A.C. Gis and Fuzzy Logic Applied to Modelling Forest Fire Risk. *An. Acad. Bras. Ciênc.* **2021**, *93*, e20190726. [CrossRef] [PubMed]
39. Lall, S.; Mathibela, B. The Application of Artificial Neural Networks for Wildfire Risk Prediction. In Proceedings of the 2016 International Conference on Robotics and Automation for Humanitarian Applications (RAHA), Kerala, India, 18–20 December 2016; pp. 1–6. [CrossRef]
40. Van Hoang, T.; Chou, T.Y.; Fang, Y.M.; Nguyen, N.T.; Nguyen, Q.H.; Xuan Canh, P.; Ngo Bao Toan, D.; Nguyen, X.L.; Meadows, M.E. Mapping Forest Fire Risk and Development of Early Warning System for NW Vietnam Using AHP and MCA/GIS Methods. *Appl. Sci.* **2020**, *10*, 4348. [CrossRef]
41. Zhao, P.; Zhang, F.; Lin, H.; Xu, S. GIS-Based Forest Fire Risk Model: A Case Study in Laoshan National Forest Park, Nanjing. *Remote Sens.* **2021**, *13*, 3704. [CrossRef]
42. Ju, W.; Xing, Z.; Wu, J.; Kang, Q. Evaluation of Forest Fire Risk Based on Multicriteria Decision Analysis Techniques for Changzhou, China. *Int. J. Disaster Risk Reduct.* **2023**, *98*, 104082. [CrossRef]
43. Abdo, H.G.; Almohamad, H.; Al Dughairi, A.A.; Al-Mutiry, M. GIS-Based Frequency Ratio and Analytic Hierarchy Process for Forest Fire Susceptibility Mapping in the Western Region of Syria. *Sustainability* **2022**, *14*, 4668. [CrossRef]
44. Çoban, H.O.; Erdin, C. Forest Fire Risk Assessment Using GIS Nad AHP Integration in Bucak Forest Enterprise, Turkey. *Appl. Ecol. Env. Res.* **2020**, *18*, 1567–1583. [CrossRef]
45. Eskandari, S. A New Approach for Forest Fire Risk Modeling Using Fuzzy AHP and GIS in Hyrcanian Forests of Iran. *Arab. J. Geosci.* **2017**, *10*, 190. [CrossRef]
46. Güngöroğlu, C. Determination of Forest Fire Risk with Fuzzy Analytic Hierarchy Process and Its Mapping with the Application of GIS: The Case of Turkey/Çakırlar. *Hum. Ecol. Risk Assess. Int. J.* **2017**, *23*, 388–406. [CrossRef]
47. Pragma; Kumar, M.; Tiwari, A.; Majid, S.I.; Bhadwal, S.; Sahu, N.; Verma, N.K.; Tripathi, D.K.; Avtar, R. Integrated Spatial Analysis of Forest Fire Susceptibility in the Indian Western Himalayas (IWH) Using Remote Sensing and GIS-Based Fuzzy AHP Approach. *Remote Sens.* **2023**, *15*, 4701. [CrossRef]
48. Goleiji, E.; Hosseini, S.M.; Khorasani, N.; Monavari, S.M. Forest Fire Risk Assessment—an Integrated Approach Based on Multicriteria Evaluation. *Env. Monit Assess* **2017**, *189*, 612. [CrossRef] [PubMed]
49. Elia, M.; D’Este, M.; Ascoli, D.; Giannico, V.; Spano, G.; Ganga, A.; Colangelo, G.; Lafortezza, R.; Sanesi, G. Estimating the Probability of Wildfire Occurrence in Mediterranean Landscapes Using Artificial Neural Networks. *Environ. Impact Assess. Rev.* **2020**, *85*, 106474. [CrossRef]
50. Estacio, J.; Narváez, N. Incendios Forestales En El Distrito Metropolitano de Quito (DMQ): Conocimiento e Intervención Pública Del Riesgo. *Let. Verdes Rev. Latinoam. De Estud. Socioambientales* **2012**, *11*, 27–52. Available online: <https://dialnet.unirioja.es/servlet/articulo?codigo=5444128> (accessed on 3 January 2024). [CrossRef]
51. Morante-Carballo, F.; Bravo-Montero, L.; Carrión-Mero, P.; Velastegui-Montoya, A.; Berrezueta, E. Forest Fire Assessment Using Remote Sensing to Support the Development of an Action Plan Proposal in Ecuador. *Remote Sens.* **2022**, *14*, 1783. [CrossRef]
52. Ramos-Rodríguez, M.P.; García-Castro, H.J.; França Tetto, A.; Carlos Batista, A.; Manrique-Toala, T.O.; Estévez-Valdés, I. Ocurrencia de Incendios Forestales En El Cantón Santa Ana, Provincia de Manabí, Ecuador (2012–2018). *Rev. Cuba. De Cienc. For.* **2021**, *9*, 322–339.
53. Reyes Bueno, F.; Balcázar Gallegos, C. Factores Que Inciden En La Probabilidad de Ocurrencia de Incendios Forestales En Ecuador. *FIGEMPA: Investig. Y Desarro.* **2021**, *11*, 50–60. [CrossRef]
54. Reyes-Bueno, F.; Loján-Córdova, J. Assessment of Three Machine Learning Techniques with Open-Access Geographic Data for Forest Fire Susceptibility Monitoring—Evidence from Southern Ecuador. *Forests* **2022**, *13*, 474. [CrossRef]
55. Servicio Nacional de Gestión de Riesgos y Emergencias. Informe de Situación No. 10 de Incendios Forestales a Nivel Nacional 2022. *Secretaría de Gestión de Riesgos 2022*. Quito, Ecuador. Available online: <https://www.gestionderiesgos.gob.ec/wp-content/uploads/downloads/2022/10/SITREP-No-10-Incendios-Forestales-01012022-a-31102022.pdf> (accessed on 25 November 2023).
56. Instituto Nacional de Estadística y Censos (INEC). Censo Ecuador 2023. *INEC 2023*. Quito, Ecuador. Available online: <https://www.censoecuador.gob.ec/> (accessed on 10 October 2023).
57. Instituto Nacional de Estadística y Censos (INEC). Censo Ecuador 2010. *INEC 2010*. Quito, Ecuador. Available online: https://www.ecuadorencifras.gob.ec/wp-content/descargas/Libros/Memorias/memorias_censo_2010.pdf (accessed on 10 October 2023).
58. Naranjo, M.; Dávalos, M.; Batallas, B.; Granja, J.; Velarde, E.; Rosales, O.; Arias, P.; Yépez, L. Proyecto Análisis de Vulnerabilidades a Nivel Municipal: Perfil Territorial Cantón San Miguel de Ibarra. *Secretaría Nacional de Gestión de Riesgos, Comisión Europea – Ayuda Humanitaria, Universidad Técnica del Norte, PNUD 2013*. Ibarra, Ecuador. Available online: <https://core.ac.uk/download/pdf/51065806.pdf> (accessed on 10 October 2023).
59. Meng, Y.; Deng, Y.; Shi, P. Mapping Forest Wildfire Risk of the World. In *World Atlas of Natural Disaster Risk*; Shi, P., Kaspersen, R., Eds.; IHDP/Future Earth-Integrated Risk Governance Project Series; Springer: Berlin/Heidelberg, Germany, 2015; pp. 261–275. ISBN 978-3-662-45429-9.

60. Cueva, E.; Lozano, D.; Yaguana, C. Efecto de La Gradiente Altitudinal Sobre La Composición Florística, Estructura y Biomasa Arbórea Del Bosque Seco Andino, Loja, Ecuador. *Bosque* **2019**, *40*, 365–378. [[CrossRef](#)]
61. Kane, V.R.; Lutz, J.A.; Alina Cansler, C.; Povak, N.A.; Churchill, D.J.; Smith, D.F.; Kane, J.T.; North, M.P. Water Balance and Topography Predict Fire and Forest Structure Patterns. *For. Ecol. Manag.* **2015**, *338*, 1–13. [[CrossRef](#)]
62. Bradstock, R.A.; Williams, R.J.; Gill, A.M. *Flammable Australia: Fire Regimes, Biodiversity and Ecosystems in a Changing World*; CSIRO Publishing: Melbourne, Australia, 2012.
63. Fearnside, P.M.; Graça, P.M.L.D.A.; Rodrigues, F.J.A. Burning of Amazonian Rainforests: Burning Efficiency and Charcoal Formation in Forest Cleared for Cattle Pasture near Manaus, Brazil. *For. Ecol. Manag.* **2001**, *146*, 115–128. [[CrossRef](#)]
64. Ward, D.E.; Susott, R.A.; Kauffman, J.B.; Babbitt, R.E.; Cummings, D.L.; Dias, B.; Holben, B.N.; Kaufman, Y.J.; Rasmussen, R.A.; Setzer, A.W. Smoke and Fire Characteristics for Cerrado and Deforestation Burns in Brazil: BASE-B Experiment. *J. Geophys. Res.* **1992**, *97*, 14601–14619. [[CrossRef](#)]
65. Kasischke, E.S.; Christensen, N.L.; Stocks, B.J. Fire, Global Warming, and the Carbon Balance of Boreal Forests. *Ecol. Appl.* **1995**, *5*, 437–451. [[CrossRef](#)]
66. Chuvieco, E.; Cocero, D.; Aguado, I.; Palacios, A.; Prado, E. Improving Burning Efficiency Estimates through Satellite Assessment of Fuel Moisture Content. *J. Geophys. Res.* **2004**, *109*, 2003JD003467. [[CrossRef](#)]
67. Maingi, J.K.; Henry, M.C. Factors Influencing Wildfire Occurrence and Distribution in Eastern Kentucky, USA. *Int. J. Wildland Fire* **2007**, *16*, 23. [[CrossRef](#)]
68. Bonora, L.; Claudio Conese, C.; Marchi, E.; Tesi, E.; Montorselli, N.B. Wildfire Occurrence: Integrated Model for Risk Analysis and Operative Suppression Aspects Management. *AJPS* **2013**, *04*, 705–710. [[CrossRef](#)]
69. Butler, B.; Anderson, W.; Catchpole, E.; Influence of Slope on Fire Spread Rate. The Fire Environment Innovations, Management, and Policy; 2007. pp. 75–83. Available online: https://www.fs.usda.gov/rm/pubs/rmrs_p046.pdf#page=85 (accessed on 10 October 2023).
70. Cardille, J.A.; Ventura, S.J.; Turner, M.G. Environmental and Social Factors Influencing Wildfires in the Upper Midwest, United States. *Ecol. Appl.* **2001**, *11*, 111–127. [[CrossRef](#)]
71. Triola, M.F. Estadística. In *Décima Edición*; Pearson Educación: Ciudad de México, México, 2004.
72. Astola, H.; Häme, T.; Sirro, L.; Molinier, M.; Kilpi, J. Comparison of Sentinel-2 and Landsat 8 Imagery for Forest Variable Prediction in Boreal Region. *Remote Sens. Environ.* **2019**, *223*, 257–273. [[CrossRef](#)]
73. Abdelkareem, O.E.A.; Elamin, H.M.A.; Eltahir, M.E.S.; Adam, H.E.; Elhaja, M.E.; Rahamtalla, A.M.; Babatunde, O.; Elmar, C. Accuracy Assessment of Land Use Land Cover in Umabdalla Natural Reserved Forest, South Kordofan, Sudan. *Int. J. Agric. Environ. Sci.* **2018**, *3*, 5–9.
74. Shao, G.; Wu, J. On the Accuracy of Landscape Pattern Analysis Using Remote Sensing Data. *Landsc. Ecol* **2008**, *23*, 505–511. [[CrossRef](#)]
75. Congalton, R.G.; Green, K. *Assessing the Accuracy of Remotely Sensed Data: Principles and Practices*; CRC Press: Boca Raton, FL, USA, 2019.
76. Ceccato, P.; Flasse, S.; Tarantola, S.; Jacquemoud, S.; Grégoire, J.-M. Detecting Vegetation Leaf Water Content Using Reflectance in the Optical Domain. *Remote Sens. Environ.* **2001**, *77*, 22–33. [[CrossRef](#)]
77. Barbosa, P.M.; Stroppiana, D.; Grégoire, J.; Cardoso Pereira, J.M. An Assessment of Vegetation Fire in Africa (1981–1991): Burned Areas, Burned Biomass, and Atmospheric Emissions. *Glob. Biogeochem. Cycles* **1999**, *13*, 933–950. [[CrossRef](#)]
78. Kogan, F.N. Remote Sensing of Weather Impacts on Vegetation in Non-Homogeneous Areas. *Int. J. Remote Sens.* **1990**, *11*, 1405–1419. [[CrossRef](#)]
79. Fick, S.E.; Hijmans, R.J. WorldClim 2: New 1-km Spatial Resolution Climate Surfaces for Global Land Areas. *Int. J. Clim.* **2017**, *37*, 4302–4315. [[CrossRef](#)]
80. Hayes, G.L. *Influence of Altitude and Aspect on Daily Variations in Factors of Forest-Fire Danger*; US Department of Agriculture: Washington, DC, USA, 1941.
81. Davis, N.N.; Badger, J.; Hahmann, A.N.; Hansen, B.O.; Mortensen, N.G.; Kelly, M.; Larsén, X.G.; Olsen, B.T.; Floors, R.; Lizcano, G.; et al. The Global Wind Atlas: A High-Resolution Dataset of Climatologies and Associated Web-Based Application. *Bull. Am. Meteorol. Soc.* **2023**, *104*, E1507–E1525. [[CrossRef](#)]
82. Thornthwaite, C.W. An Approach toward a Rational Classification of Climate. *Geogr. Rev.* **1948**, *38*, 55–94. [[CrossRef](#)]
83. Thornthwaite, C.; Matter, J. *The Water Balance*; Publication in Climatology; Drexel Institute of Technology: Centerton, NJ, USA, 1955.
84. Saaty, T.L. *The Analytic Hierarchy Process: Planning, Priority Setting, Resource Allocation*; Thomas, L., Ed.; SAATY McGraw-Hill: New York, NY, USA, 1980.
85. Sinha, A.; Nikhil, S.; Ajin, R.S.; Danumah, J.H.; Saha, S.; Costache, R.; Rajaneesh, A.; Sajinkumar, K.S.; Amrutha, K.; Johnny, A.; et al. Wildfire Risk Zone Mapping in Contrasting Climatic Conditions: An Approach Employing AHP and F-AHP Models. *Fire* **2023**, *6*, 44. [[CrossRef](#)]
86. Lee, S.; Choi, J.; Woo, I. The Effect of Spatial Resolution on the Accuracy of Landslide Susceptibility Mapping: A Case Study in Boun, Korea. *Geosci. J.* **2004**, *8*, 51–60. [[CrossRef](#)]
87. Beguería, S. Validation and Evaluation of Predictive Models in Hazard Assessment and Risk Management. *Nat. Hazards.* **2006**, *37*, 315–329. [[CrossRef](#)]

88. Pradhan, B.; Lee, S. Landslide Susceptibility Assessment and Factor Effect Analysis: Backpropagation Artificial Neural Networks and Their Comparison with Frequency Ratio and Bivariate Logistic Regression Modelling. *Environ. Model. Softw.* **2010**, *25*, 747–759. [[CrossRef](#)]
89. Jaiswal, R.K.; Mukherjee, S.; Raju, K.D.; Saxena, R. Forest Fire Risk Zone Mapping from Satellite Imagery and GIS. *Int. J. Appl. Earth Obs. Geoinf.* **2002**, *4*, 1–10. [[CrossRef](#)]
90. Narayanaraj, G.; Wimberly, M.C. Influences of Forest Roads on the Spatial Patterns of Human- and Lightning-Caused Wildfire Ignitions. *Appl. Geogr.* **2012**, *32*, 878–888. [[CrossRef](#)]
91. Zambon, I.; Cerdà, A.; Cudlin, P.; Serra, P.; Pili, S.; Salvati, L. Road Network and the Spatial Distribution of Wildfires in the Valencian Community (1993–2015). *Agriculture* **2019**, *9*, 100. [[CrossRef](#)]
92. Balslev, H.; Luteyn, J.L. Páramo: An Andean Ecosystem under Human Influence. In *Paramo: An Andean Ecosystem under Human Influence*; Academic Press: Cambridge, MA, USA, 1992; Available online: <https://pure.au.dk/portal/en/publications/paramo-an-andean-ecosystem-under-human-influence> (accessed on 26 October 2023).
93. Buytaert, W.; Célleri, R.; De Bièvre, B.; Cisneros, F. Hidrología Del Páramo Andino: Propiedades, Importancia y Vulnerabilidad. Cuenca. 2006. Available online: http://www.paramo.org/files/hidrologia_paramo.pdf (accessed on 25 October 2023).
94. Célleri Alvear, R.; Crespo Sánchez, P.; Mosquera, G.M.; Ochoa-Sánchez, A.E.; Pesántez Vallejo, J.P. Hidrología de los páramos en el Ecuador. In *Los Páramos del Ecuador: Pasado, Presente y Futuro*; Universidad San Francisco de Quito (USFQ) Press: Quito, Ecuador, 2023; pp. 76–101. ISBN 978-9978-68-264-7. [[CrossRef](#)]
95. Matthews, S. Effect of Drying Temperature on Fuel Moisture Content Measurements. *Int. J. Wildland Fire* **2010**, *19*, 800–802. [[CrossRef](#)]
96. Herawati, H.; Santoso, H. Tropical Forest Susceptibility to and Risk of Fire under Changing Climate: A Review of Fire Nature, Policy and Institutions in Indonesia. *For. Policy Econ.* **2011**, *13*, 227–233. [[CrossRef](#)]
97. Alcasena, F.J.; Ager, A.A.; Bailey, J.D.; Pineda, N.; Vega-García, C. Towards a Comprehensive Wildfire Management Strategy for Mediterranean Areas: Framework Development and Implementation in Catalonia, Spain. *J. Environ. Manag.* **2019**, *231*, 303–320. [[CrossRef](#)]
98. Zong, X.; Tian, X.; Fang, L. Assessing Wildfire Risk and Mitigation Strategies in Qipanshan, China. *Int. J. Disaster Risk Reduct.* **2022**, *80*, 103237. [[CrossRef](#)]
99. Yathish, H.; Athira, K.V.; Preethi, K.; Pruthviraj, U.; Shetty, A. A Comparative Analysis of Forest Fire Risk Zone Mapping Methods with Expert Knowledge. *J. Indian Soc. Remote Sens.* **2019**, *12*, 2047–2060. [[CrossRef](#)]
100. Zubietta, R.; Prudencio, F.; Ccanchi, A.B.Y.; Saavedra, M.; Sulca, J.; Reupo, J.; Alarco, G. Potential Conditions for Fire Occurrence in Vegetation in the Peruvian Andes. *Int. J. Wildland Fire* **2021**, *30*, 836–849. [[CrossRef](#)]
101. Hamilton, A.T.; Schäfer, R.B.; Pyne, M.I.; Chessman, B.; Kakouei, K.; Boersma, K.S.; Verdonshot, P.F.M.; Verdonshot, R.C.M.; Mims, M.; Khamis, K.; et al. Limitations of Trait-Based Approaches for Stressor Assessment: The Case of Freshwater Invertebrates and Climate Drivers. *Glob. Change Biol.* **2020**, *26*, 364–379. [[CrossRef](#)]

Disclaimer/Publisher’s Note: The statements, opinions and data contained in all publications are solely those of the individual author(s) and contributor(s) and not of MDPI and/or the editor(s). MDPI and/or the editor(s) disclaim responsibility for any injury to people or property resulting from any ideas, methods, instructions or products referred to in the content.